



## $\alpha$ -Selinene from *Syzygium aqueum* against Aromatase p450 in Breast Carcinoma of Postmenopausal Women: in Silico Study

Oluwaseun Suleiman Alakanse<sup>1\*</sup>, Faoziyat Adenike Sulaiman<sup>1</sup>, Abiodun Julius Arannilewa<sup>1,2</sup>, Funmilola Favour Anjorin<sup>3</sup>, Oluwaseyi Israel Malachi<sup>4</sup>, Ibukunoluwa Ebunolorun Ayo<sup>2</sup>, Afees Adebayo Oladejo<sup>5</sup>, Olutekunbi Akinwumi Oluwole<sup>6</sup>, Opaleye Oyetola Olanrewaju<sup>1</sup>, Usman Okeme<sup>1</sup>, Ambrose Oche George<sup>1</sup>, Acho Marvellous Amarachi<sup>1</sup>, Oluwaseun Oluwatosin Taofeek<sup>1</sup>, Olufemi Samuel Araoyinbo<sup>7</sup>, Ayobamidele Abass Bakare<sup>6</sup> and Tolulope Oluwafemi Bolarinwa<sup>6</sup>

<sup>1</sup>Department of Biochemistry, University of Ilorin, Ilorin, Nigeria

<sup>2</sup>Department of Biochemistry, Ekiti State University, Ado-Ekiti, Nigeria

<sup>3</sup>Department of Chemical Pathology, University of Ibadan, Nigeria

<sup>4</sup>Food Production Department, Good Foods Inc., Montreal, QC, Canada

<sup>5</sup>Applied Biochemistry Department, Nnamdi Azikiwe University, Awka, Nigeria

<sup>6</sup>Department of Biochemistry, Federal University of Technology, Akure, Nigeria

<sup>7</sup>Department of Chemistry, university of Ibadan, Ibadan, Nigeria

### Abstract

Breast cancer is the most diagnosed and prevalent cancer in women both in developed and developing countries, this constitutes a threat to the society and world economic stability. *In situ* carcinoma and invasive carcinoma are the broad rubric of breast cancer. In established breast carcinoma, about 80% depends on the gird of estrogen hormone for growth. Hence, the down-regulation of aromatase activities has been one of the strategies used in the treatment of breast-related carcinomas.

This study explores *Syzygium aqueum* for the best drug-gable compound via computation tools. Seventy-one compounds were obtained from *Syzygium aqueum* plant which was retrieved from works of literature and were docked into the active site of aromatase p450 for their antagonistic effects. A-selinene, the lead compound with the binding energy of -8.5 kcal/mol was obtained using PyRx, autodock vina tools used in the molecular docking to obtain the docking scores. To ensure and validate that the right target was used, the FASTA sequence of the crystalline structure of aromatase p450 was blast on the chembl database.

Spearman rank correlation coefficient graph was plotted on graphpad prism 6 to obtain a strong correlation ( $R^2$ ) value of 0.77 between the dockings results of the ChEMBL'S compounds and their corresponding experimentally generated IC50 results. These results explain why  $\alpha$ -selinene should be considered a potential antagonist of aromatase p450 in postmenopausal women suffering from breast carcinomas.

**Keywords:** Aromatase p450;  $\alpha$ -Selinene; Breast cancer; CYP19A1 gene; NADPH cytochrome p450 reductase; Androgens; Estrogens

### Introduction

Cancer is a malignant disease condition emerging from uncontrollable cell division in the body to form mass of tissues. The cells have the capacity to metastasize; that is infiltrate adjacent or distant site in the body where they proliferate uncontrollably thus, causing significant mortality and morbidity [1].

According to the world health organization, 55% of women worldwide are overweight or obese [2]. Breast cancer is the most diagnosed cancer in women in developed and developing countries. Breast cancer in female is the most prevalent cancer in developing and developed countries; hence constitute a treat to the society and world economic stability. *In situ* carcinoma and invasive carcinoma are the broad rubric of breast cancer. Carcinoma *in situ* is further subdivided as either ductal carcinoma *in situ* (DCIS) or lobular cancer *in situ* (LCIS). While the two categories of DCIS are; comedocarcinoma and non-comedocarcinoma. In addition to this, the major invasive tumor types include invasive lobular (ILC) or invasive ductal carcinoma (IDC) which accounts for 70-80% of all invasive lesions [3-6].

DNA microarrays analysis sub-classified breast cancer into, luminal a: which is positive for ER, negative for HER2, low Ki-67 protein and high PR. Luminal b: which is positive for ER, negative for HER2, and either Ki-67 protein high or PR low, basal-like breast cancer: this

lacks expression of the molecular targets that confer responsiveness to highly effective targeted therapies such as Tamoxifen and Aromatase inhibitors), Triple-negative breast cancer (TNBC) (ER-, PR-, and HER2-negative tumors), HER2+: (ERBB2+) has amplified HER2/neu. HER2-positive cancer is diagnosed in 10%–20% of breast cancer patients, which is particularly aggressive and more likely to spread rapidly than other types of breast cancer, claudin low (often TN, but distinct in that, there is low expression of cell–cell junction proteins including e-cadherin and are commonly infiltrated with lymphocytes) [7,8].

In established breast carcinoma, about 80%, depends on accouter of estrogen hormone for growth, hence, estrogen receptor positive (ER)

**\*Corresponding author:** Oluwaseun Suleiman Alakanse, Department of Biochemistry, University of Ilorin, Ilorin, Nigeria, Tel: +2348102595628; E-mail: [oluwaseunalakanse@gmail.com](mailto:oluwaseunalakanse@gmail.com)

**Received:** November 12, 2018; **Accepted:** December 04, 2018; **Published:** January 03, 2019

**Citation:** Alakanse OS, Sulaiman FA, Arannilewa AJ, Anjorin FF, Malachi OI, et al. (2019)  $\alpha$ -Selinene from *Syzygium aqueum* against Aromatase p450 in Breast Carcinoma of Postmenopausal Women: in Silico Study. J Biomed Pharm Sci 1: 116.

**Copyright:** © 2019 Alakanse OS, et al. This is an open-access article distributed under the terms of the Creative Commons Attribution License, which permits unrestricted use, distribution, and reproduction in any medium, provided the original author and source are credited.

carcinoma. Estrogens pioneer neoplastic growth via binding to their receptors in the tumor Figure 1. In premenopausal women, the source of estrogen is the ovaries, while the skin, adipose tissue and the breast are the main source of estrogen in post-menopausal women. Hence, hormone therapy; that's the down-regulation of aromatase activities as been one of the strategies used in the treatment of breast related carcinomas [9,10].

Human aromatase enzyme, located in the endoplasmic reticulum, a member of the cytochrome p450 family and translational product of the CYP19A1 gene, located on chromosome 15 [11,12], a key enzyme required for the biosynthesis of estrogens. Aromatase is an heterodimer enzyme, in that it is made up of a ubiquitous NADPH cytochrome p450 reductase and cytochrome 450 aromatase; whose catalytic portion contains a heme group and a steroid binding site [13]. It catalyzes the rate-limiting step and the aromatization of androgens to estrogens Figure 2. The bimolecular reaction of aromatase is carried out in three oxidation reactions of the androstenedione a ring, in which each reaction utilize a molecule of both oxygen and NADPH. The first two reaction steps are common to p450 cytochrome proteins, while the third is unique to aromatase [14]. Carcinomas of the breast have been shown to express aromatase, which consequently leads to higher levels of estrogens than non-cancerous cells and the core reason why aromatase generates a high level of interest for the treatment of breast cancer [15].

The standard treatments for postmenopausal women with hormone receptor-positive breast cancer are the AIs. Been effective treatment for hormone receptor-positive breast cancer, their benefit is often circumscribed by emergence and interference of resistance which occurs in adjuvant setting and in metastatic breast cancer Figure 3. The two distinct pathways involved in resistance include ER signalling and growth factor receptor pathways. Carcinomas of the breast that either expresses ER or PR are known to be non-respondent to endocrinotherapeutic effects of AIs which is other way round for patients with higher levels of ER or PR level [16-18].

Water jamba (*Syzygium aqueum*), ethnomedically, water jamba plant parts have varied applications which includes, antibiotic activity, antifissures tongue, itching reliever, antiturgescence, antioxidant, antityrosinase, anticellulite activities, lipolytics, antihyperglycemic ( $\alpha$ -glucosidase,  $\alpha$ -amylases, advanced glycation end products (AGEs) and aldose reductase (AR) inhibitory activities). *Syzygium aqueum* aldose reductase inhibitory activity has been reported to reduce

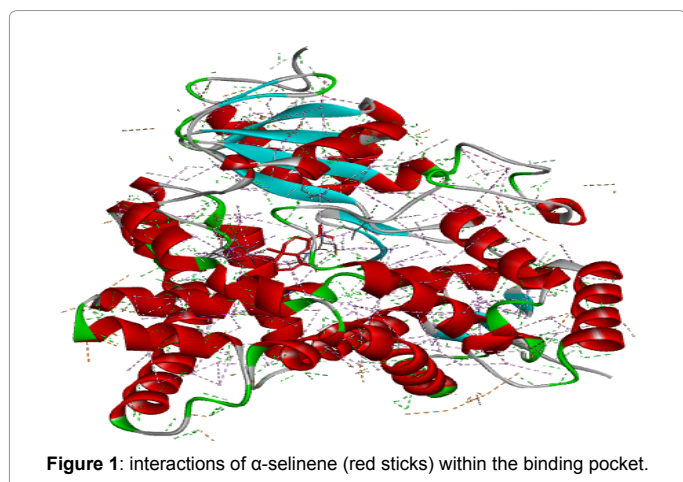


Figure 1: interactions of  $\alpha$ -selinene (red sticks) within the binding pocket.

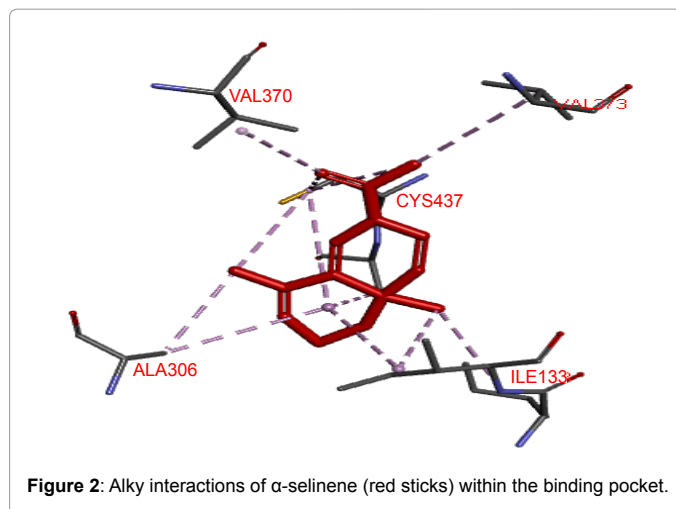


Figure 2: Alky interactions of  $\alpha$ -selinene (red sticks) within the binding pocket.

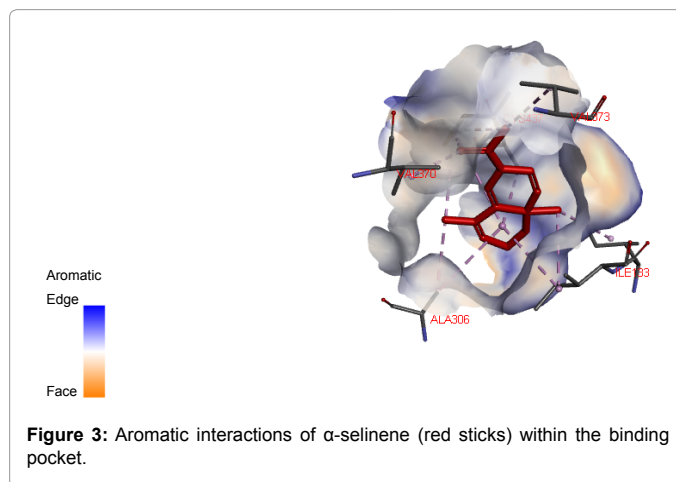


Figure 3: Aromatic interactions of  $\alpha$ -selinene (red sticks) within the binding pocket.

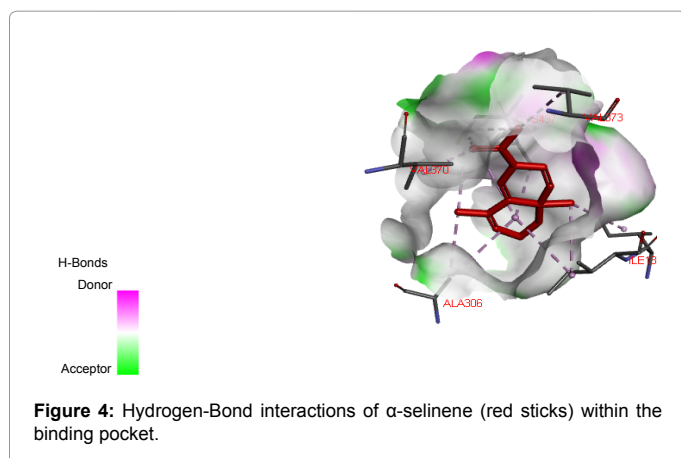
microvascular complication of diabetes which includes retinopathy, nephropathy, neuropathy and cataracts [19-23].

Irreversible steroidal inhibitors (exemestane and formestane) and non-steroidal inhibitors (anastrozole and letrozole) are the two types of aromatase inhibitors approved for the treatment of hormonally-responsive breast cancer in postmenopausal women, since they had been proven to be superior to tamoxifene known as a representative of selective estrogen receptor modulators (SERMs). Pharmacotherapies (AIs), with distinct pharmacokinetics and pharmacodynamics properties, and other orthodox methods used in the treatment of postmenopausal ER+ breast cancer as lead to varied pathophysiological contradictions such as; osteoporosis, osteopenia, arthralgia, myalgia, hot flashes, night sweats and vaginal dryness. Hence, a need for the discovery of more potent, efficient, cost-effective active principles of plant origin with little or no side effects which are capable to alleviate a/s complications [24-29].

## Materials and Methods

### Ligand selection and preparation

Seventy-one (71) phytochemical of *Syzygium aqueum* plant were retrieved from pubchem compound database (<https://pubchem.ncbi>).



nlm.nih.gov). The MOL SDF format of these ligands were converted to PDBQT file using PyRx tool to generate atomic coordinates and energy was minimized by using the optimization algorithm at force field set at mmff (required) on PyRx Figure 4.

#### Accession and preparation of the target protein

The three-dimension crystal structure of aromatase p450 (PDB: 5jkv) in complex with a co-crystallized ligand was retrieved from RCSB PDB (<http://www.rcsb.org/pdb/home/home.do>) [8]. Pymol tool was used to clean the protein by removing non-essential water molecules and all heteroatoms that complex with the protein. The grid coordinate around the active site was revealed by the extraction of the ligand.

#### Molecular docking using PyRx

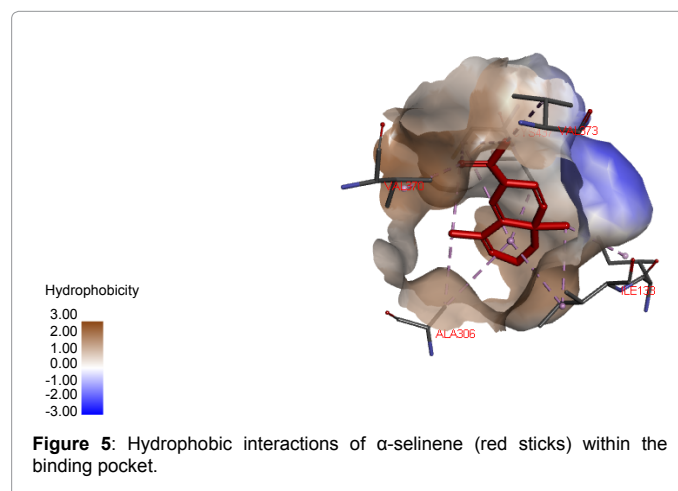
For our analysis we used the PyRx, autodock vina exhaustive search docking function. After the minimization process, the grid box resolution was centered at  $83.4520 \times 50.1752 \times 46.4060$  along the x, y and z axes respectively at grid dimension of  $25 \times 25 \times 25 \text{ \AA}$  to define the binding site. The co-crystallized ligand which serves as the standard was first docked within the binding site of aromatase p450 and the resulting interaction was compared with that of  $\alpha$ -selinene into the similar active sites using the same grid box dimension.

#### Validation of docking results

Validation of the docking score obtained was carried out by blasting the FASTA sequence of the crystalline structure of aromatase p450 which was obtained from protein data bank unto the online available ChEMBL database ([www.ebi.ac.uk/chembl/](http://www.ebi.ac.uk/chembl/)). The bioactivity generated by the database, having an inhibition of 959 and IC<sub>50</sub> value of 2617, was downloaded in txt format. The bioactivity was sorted out; missing or misplaced data were removed. Only 28 of the total 2617 drug-like compounds were recovered. The compiled compounds were split and converted to 2d (in SDF format) by Datawarrior software (version 2) and converted to PDBQT format by PyRx tool. The ligands were docked into the binding domain of aromatase p450 using PyRx Autodock Vina scoring function. A correlation coefficient graph was plotted between the docking scores of the 28 compounds generated and their corresponding PCHEMBL\_VALUE (experimentally determined) values. Spearman rank correlation coefficient graph was plotted on graphpad prism 6 to obtain a strong correlation ( $R^2$ ) value between the dockings results of the ChEMBLs compounds and their corresponding experimentally generated IC<sub>50</sub> results Figure 5.

## Results and Discussion

CYP19A1 gene located on chromosome 15 synthesizes the heterodimer aromatase p450, a key enzyme required for the biosynthesis



Ligand	Binding Energy	Binding Affinity	Rmsd/ub	Rmsd/lb
Standard_0	E=373.82	-7.7	0	0
Compound_1	E=13.90	-5.9	0	0
Compound_2	E=97.17	-4.2	0	0
Compound_3	E=25.69	-6.4	0	0
Compound_4	E=67.31	-5.2	0	0
Compound_5	E=3.07	-4.5	0	0
Compound_6	E=-3.74	-4.3	0	0
Compound_7	E=223.31	-5.8	0	0
Compound_8	E=49.72	-3.8	0	0
Compound_9	E=677.22	-5	0	0
Compound_10	E=19.61	-5.8	0	0
Compound_11	E=148.71	-6.2	0	0
Compound_12	E=140.00	-6	0	0
Compound_13	E=140.20	-6.1	0	0
Compound_14	E=22.68	-6.1	0	0
Compound_15	E=14.00	-5.5	0	0
Compound_16	E=22.39	-5	0	0
Compound_17	E=18.92	-6.2	0	0
Compound_18	E=17.62	-5.5	0	0
Compound_19	E=-2.31	-4.7	0	0
Compound_20	E=-2.38	-4.7	0	0
Compound_21	E=-30.24	-4	0	0
Compound_22	E=11.80	-4.9	0	0
Compound_23	E=-0.15	-5.3	0	0
Compound_24	E=13.24	-5.2	0	0
Compound_25	E=-1.59	-5	0	0
Compound_26	E=18.23	-4.3	0	0
Compound_27	E=648.80	-6	0	0
Compound_28	E=41.86	-4.1	0	0
Compound_29	E=140.67	-6.1	0	0
Compound_30	E=43.08	-4.1	0	0
Compound_31	E=-0.11	-3.4	0	0
Compound_33	E=30.12	-5.2	0	0
Compound_32	E=315.62	-6.5	0	0

Compound_34	E=70.37	-6.2	0	0
Compound_35	E=31.40	-5.9	0	0
Compound_36	E=17.42	-4.3	0	0
Compound_37	E=8.84	-4.8	0	0
Compound_38	E=385.28	-6.3	0	0
Compound_39	E=1161.81	-8.1	0	0
Compound_40	E=204.01	-6.2	0	0
Compound_41	E=138.34	-6.1	0	0
Compound_42	E=167.47	-7.9	0	0
Compound_43	E=1308.26	-8.4	0	0
Compound_44	E=2.61	-4.9	0	0
Compound_45	E=-4.35	-5.7	0	0
Compound_46	E=15.11	-5.4	0	0
Compound_47	E=15.60	-4.7	0	0
Compound_48	E=5.23	-5	0	0
Compound_49	E=2.69	-5	0	0
Compound_50	E=203.42	-8.4	0	0
Compound_51	E=44.06	-6.9	0	0
Compound_52	E=30.91	-5.7	0	0
Compound_53	E=2.68	-5.2	0	0
Compound_54	E=1.12	-5	0	0
Compound_55	E=2.28	-5.7	0	0
Compound_56	E=-1.59	-5	0	0
Compound_57	E=-1.17	-4.8	0	0
Compound_58	E=1.09	-5.3	0	0
Compound_59	E=12.43	-4.9	0	0
Compound_60	E=192.35	-6.1	0	0
Compound_61	E=29.96	-5	0	0
Compound_62	E=16.37	-5.4	0	0
Compound_63	E=62.20	-7	0	0
Compound_64	E=404.73	-6.8	0	0
Compound_65	E=385.28	-6.3	0	0
Compound_66	E=159.61	-6.1	0	0
Compound_68	E=93.38	-6.5	0	0
Compound_69	E=70.37	-6.2	0	0
Compound_70	E=318.85	-8.5	0	0
Compound_71	E=884.29	-8.1	0	0

**Table 1:** Interaction table showing the various chemical interactions of  $\alpha$ -selinene within the binding pocket (Viewed on Discovery studio Visualizer).

of estrogens. It catalyzes the rate-limiting step and the aromatization of androgens to estrogens Table 1. Carcinomas of the breast have been shown to express aromatase, which consequently leads to higher levels of estrogens than non-cancerous cells and the core reason why aromatase generates a high level of interest for the treatment of breast cancer.

In the present studies, seventy-one (71) phytocompounds from *Syzygium aqueum* plant were docked into the binding pocket of aromatase p450 for their antagonistic properties.  $\alpha$ -selinene, the lead compound with the binding energy of -8.5 kcal/mol compared to the standard (-7.7 kcal/mol). The drug-likeness properties of  $\alpha$ -selinene violated none of the lipinski's rule of five, and this describes the binding potential and bioavailability of  $\alpha$ -selinene.

The highest binding energy attributed to  $\alpha$ -selinene is believed to be due to the strong interaction at the active site, which includes; electrostatic, hydrogen, and hydrophobic interaction (Table 2 Figure 6).

1) Thirty-six hydrogen bond interactions which involves; ARG 115, 145, 375, 435, ILE 133, 132, ARG 435, GLU 302, TRP 141, GLY 436,

439, PHE 148, 430, LEU 152, ALA 306, 307, GLU 302, 439, THR 310, CYS 437

2) Fifty-four hydrophobic interactions which involves; ILE 132, 133, PHE 148, 430, ARG 145, 435, ALA 306, 438, CYS 437, LEU 162, 437, VAL 373, 370, TRP 141, MET 303

3) Four electrostatic interactions which involves; ARG 415 and TRP 141

While the standard as the following interaction at the binding pocket which involves;

4) Six hydrogen interactions which involves MET 311, ALA 307, 443, CYS 437, PHE 430 and GLY 439

5) Twenty-two interaction hydrophobic interactions which involves ALA 306, 307, 443, MET 311, CYS 437, VAL 370, PHE 430 (Table 3).

The highest binding energy (-8.5 kcal/mol) attributed to  $\alpha$ -selinene is believed to be as a result of the extensive high number of hydrophobic interaction of  $\alpha$ -selinene with the pocket binding site. The average number of hydrophobic atoms in marketed drugs is 16, with one or two donors and three to four acceptors. This depicts the importance of hydrophobic interaction in the design of drugs. This further explains the high binding affinity of between target-drug interfaces. The dependability of our docking scores was further confirmed using the ChEMBL database. The compounds obtained from aromatase p450 FASTA sequence blast were docked into the binding pocket of aromatase p450; a strong correlation coefficient of 0.77 was obtained

S/N	Complex	Binding energy (From PyRx)	RMSD/UB <sup>a</sup>	RMSD/LB <sup>b</sup>
70	Alpha-Selinene (10856614)	-8.5	0	0
50	Caryophyllene (5281515)	-8.4	0	0
43	Beta-selinene (442393)	-8.4	0	0
39	Alpha-cabebene (88609)	-8.1	0	0
71	Bicyclogermacrene	-8.1	0	0
0	Standard	-7.7	0	0

RMSD/UB: Root mean square deviation/upper bond; RMSD/LB: Root mean square deviation/lower bond

**Table 2:** Interaction table showing  $\alpha$ -Selinene of the five chemical compounds with highest binding energy within the binding pocket (Viewed on Discovery studio Visualizer)

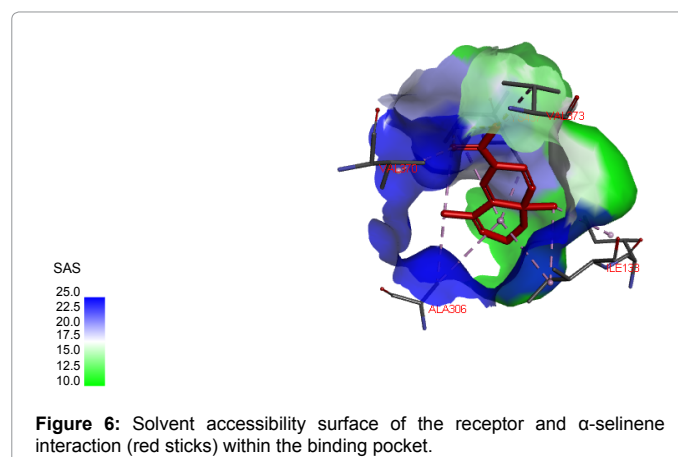


**Figure 6:** Solvent accessibility surface of the receptor and  $\alpha$ -selinene interaction (red sticks) within the binding pocket.

Name	Category	Types
A:ARG115:HE - A:ILE133:O	Hydrogen Bond	Conventional Hydrogen Bond
A:ARG115:HH21 - A:ARG435:O	Hydrogen Bond	Conventional Hydrogen Bond
A:ILE132:HN - A:GLU302:OE1	Hydrogen Bond	Conventional Hydrogen Bond
A:ILE133:HN - A:GLU302:OE1	Hydrogen Bond	Conventional Hydrogen Bond
A:ARG145:HN - A:TRP141:O	Hydrogen Bond	Conventional Hydrogen Bond
A:ARG145:HH11 - A:GLY436:O	Hydrogen Bond	Conventional Hydrogen Bond
A:ARG145:HH21 - A:GLY436:O	Hydrogen Bond	Conventional Hydrogen Bond
A:PHE148:HN - A:ARG145:O	Hydrogen Bond	Conventional Hydrogen Bond
A:LEU152:HN - A:PHE148:O	Hydrogen Bond	Conventional Hydrogen Bond
A:ALA306:HN - A:GLU302:O	Hydrogen Bond	Conventional Hydrogen Bond
A:THR310:HN - A:ALA306:O	Hydrogen Bond	Conventional Hydrogen Bond
A:THR310:HN - A:ALA307:O	Hydrogen Bond	Conventional Hydrogen Bond
A:ARG375:HH22 - A:ARG435:O	Hydrogen Bond	Conventional Hydrogen Bond
A:ARG435:HH22 - A:ILE132:O	Hydrogen Bond	Conventional Hydrogen Bond
A:ARG435:HH22 - A:ILE133:O	Hydrogen Bond	Conventional Hydrogen Bond
A:CYS437:HN - A:PHE430:O	Hydrogen Bond	Conventional Hydrogen Bond
A:GLY439:HN - A:CYS437:SG	Hydrogen Bond	Conventional Hydrogen Bond
A:TRP141:CD1 - A:ILE132:O	Hydrogen Bond	Carbon Hydrogen Bond
A:ARG435:NH1 - A:TRP141	Electrostatic	Pi-Cation
A:ARG435:NH1 - A:TRP141	Electrostatic	Pi-Cation
A:ILE132:CD1 - A:PHE148	Hydrophobic	Pi-Sigma
A:ILE133 - N:UNK1	Hydrophobic	Alkyl
A:ARG145 - A:ILE132	Hydrophobic	Alkyl
A:ALA306 - N:UNK1	Hydrophobic	Alkyl
A:ALA306 - N:UNK1:C	Hydrophobic	Alkyl
A:CYS437 - N:UNK1	Hydrophobic	Alkyl
A:ALA438 - A:LEU152	Hydrophobic	Alkyl
A:ALA438 - N:UNK1	Hydrophobic	Alkyl
N:UNK1:C - A:CYS437	Hydrophobic	Alkyl
N:UNK1:C - A:ILE132	Hydrophobic	Alkyl
N:UNK1:C - A:ILE133	Hydrophobic	Alkyl
N:UNK1:C - A:VAL370	Hydrophobic	Alkyl
N:UNK1:C - A:CYS437	Hydrophobic	Alkyl
N:UNK1:C - A:VAL373	Hydrophobic	Alkyl
N:UNK1:C - A:CYS437	Hydrophobic	Alkyl
A:TRP141 - A:ILE132	Hydrophobic	Pi-Alkyl
A:TRP141 - A:ARG145	Hydrophobic	Pi-Alkyl
A:TRP141 - A:ARG435	Hydrophobic	Pi-Alkyl
A:TRP141 - A:ARG435	Hydrophobic	Pi-Alkyl
A:PHE148 - A:MET303	Hydrophobic	Pi-Alkyl
A:PHE430 - A:CYS437	Hydrophobic	Pi-Alkyl
A:ILE133 - N:UNK1	Hydrophobic	Alkyl
A:ALA306 - N:UNK1	Hydrophobic	Alkyl
A:ALA306 - N:UNK1:C	Hydrophobic	Alkyl
A:CYS437 - N:UNK1	Hydrophobic	Alkyl
A:ALA438 - N:UNK1	Hydrophobic	Alkyl
N:UNK1:C - A:CYS437	Hydrophobic	Alkyl
N:UNK1:C - A:ILE132	Hydrophobic	Alkyl
N:UNK1:C - A:ILE133	Hydrophobic	Alkyl
N:UNK1:C - A:VAL370	Hydrophobic	Alkyl
N:UNK1:C - A:CYS437	Hydrophobic	Alkyl
N:UNK1:C - A:VAL373	Hydrophobic	Alkyl
N:UNK1:C - A:CYS437	Hydrophobic	Alkyl
A:ARG115:HE - A:ILE133:O	Hydrogen Bond	Conventional Hydrogen Bond
A:ARG115:HH21 - A:ARG435:O	Hydrogen Bond	Conventional Hydrogen Bond
A:ILE132:HN - A:GLU302:OE1	Hydrogen Bond	Conventional Hydrogen Bond

A:ILE133:HN - A:GLU302:OE1	Hydrogen Bond	Conventional Hydrogen Bond
A:ARG145:HN - A:TRP141:O	Hydrogen Bond	Conventional Hydrogen Bond
A:ARG145:HH11 - A:GLY436:O	Hydrogen Bond	Conventional Hydrogen Bond
A:ARG145:HH21 - A:GLY436:O	Hydrogen Bond	Conventional Hydrogen Bond
A:PHE148:HN - A:ARG145:O	Hydrogen Bond	Conventional Hydrogen Bond
A:LEU152:HN - A:PHE148:O	Hydrogen Bond	Conventional Hydrogen Bond
A:ALA306:HN - A:GLU302:O	Hydrogen Bond	Conventional Hydrogen Bond
A:THR310:HN - A:ALA306:O	Hydrogen Bond	Conventional Hydrogen Bond
A:THR310:HN - A:ALA307:O	Hydrogen Bond	Conventional Hydrogen Bond
A:ARG375:HH22 - A:ARG435:O	Hydrogen Bond	Conventional Hydrogen Bond
A:ARG435:HH22 - A:ILE132:O	Hydrogen Bond	Conventional Hydrogen Bond
A:ARG435:HH22 - A:ILE133:O	Hydrogen Bond	Conventional Hydrogen Bond
A:CYS437:HN - A:PHE430:O	Hydrogen Bond	Conventional Hydrogen Bond
A:GLY439:HN - A:CYS437:SG	Hydrogen Bond	Conventional Hydrogen Bond
A:TRP141:CD1 - A:ILE132:O	Hydrogen Bond	Carbon Hydrogen Bond
A:ARG435:NH1 - A:TRP141	Electrostatic	Pi-Cation
A:ARG435:NH1 - A:TRP141	Electrostatic	Pi-Cation
A:ILE132:CD1 - A:PHE148	Hydrophobic	Pi-Sigma
A:ILE133 - N:UNK1	Hydrophobic	Alkyl
A:ARG145 - A:ILE132	Hydrophobic	Alkyl
A:ALA306 - N:UNK1	Hydrophobic	Alkyl
A:ALA306 - N:UNK1:C	Hydrophobic	Alkyl
A:CYS437 - N:UNK1	Hydrophobic	Alkyl
A:ALA438 - A:LEU152	Hydrophobic	Alkyl
A:ALA438 - N:UNK1	Hydrophobic	Alkyl
N:UNK1:C - A:CYS437	Hydrophobic	Alkyl
N:UNK1:C - A:ILE132	Hydrophobic	Alkyl
N:UNK1:C - A:ILE133	Hydrophobic	Alkyl
N:UNK1:C - A:VAL370	Hydrophobic	Alkyl
N:UNK1:C - A:CYS437	Hydrophobic	Alkyl
N:UNK1:C - A:VAL373	Hydrophobic	Alkyl
N:UNK1:C - A:CYS437	Hydrophobic	Alkyl
A:TRP141 - A:ILE132	Hydrophobic	Pi-Alkyl
A:TRP141 - A:ARG145	Hydrophobic	Pi-Alkyl
A:TRP141 - A:ARG435	Hydrophobic	Pi-Alkyl
A:TRP141 - A:ARG435	Hydrophobic	Pi-Alkyl
A:PHE148 - A:MET303	Hydrophobic	Pi-Alkyl
A:PHE430 - A:CYS437	Hydrophobic	Pi-Alkyl

**Table 3:** Interaction table showing the various chemical interactions of  $\alpha$ -Selinene within the binding pocket.

Name	Category	Types
A:MET311:HN - A:ALA307:O	Hydrogen Bond	Conventional Hydrogen Bond
A:CYS437:HN - A:PHE430:O	Hydrogen Bond	Conventional Hydrogen Bond
A:GLY439:HN - A:CYS437:SG	Hydrogen Bond	Conventional Hydrogen Bond
A:ALA443:HN - A:GLY439:O	Hydrogen Bond	Conventional Hydrogen Bond
A:GLY439:CA - N:ASD602:O	Hydrogen Bond	Carbon Hydrogen Bond
A:ALA306 - N:ASD602	Hydrophobic	Alkyl
A:ALA307 - A:MET311	Hydrophobic	Alkyl
A:ALA307 - N:ASD602:C	Hydrophobic	Alkyl
A:CYS437 - N:ASD602	Hydrophobic	Alkyl
A:CYS437 - N:ASD602	Hydrophobic	Alkyl
A:ALA443 - A:MET311	Hydrophobic	Alkyl
A:ALA443 - N:ASD602	Hydrophobic	Alkyl
A:ALA443 - N:ASD602	Hydrophobic	Alkyl
N:ASD602:C - A:VAL370	Hydrophobic	Alkyl
N:ASD602:C - A:MET311	Hydrophobic	Alkyl

A:PHE430 - A:CYS437	Hydrophobic	Pi-Alkyl
A:PHE430 - A:ALA443	Hydrophobic	Pi-Alkyl
A:PHE430 - N:ASD602	Hydrophobic	Pi-Alkyl
A:GLY439:CA - N:ASD602:O	Hydrogen Bond	Carbon Hydrogen Bond
A:ALA306 - N:ASD602	Hydrophobic	Alkyl
A:ALA307 - N:ASD602:C	Hydrophobic	Alkyl
A:CYS437 - N:ASD602	Hydrophobic	Alkyl
A:CYS437 - N:ASD602	Hydrophobic	Alkyl
A:ALA443 - N:ASD602	Hydrophobic	Alkyl
A:ALA443 - N:ASD602	Hydrophobic	Alkyl
N:ASD602:C - A:VAL370	Hydrophobic	Alkyl
N:ASD602:C - A:MET311	Hydrophobic	Alkyl
A:PHE430 - N:ASD602	Hydrophobic	Pi-Alkyl

**Table 4:** Interaction table showing the chemical interaction of the co-crystallized ligand within the binding pocket.

Lipinski's Rule of Drug Evaluation $\alpha$ -selinene	
MW<=500	204.357
Hacc<=10	0
Hdon<=5	0
Log P<=5	4.725
MR <=	66.743
TPSA<=140	0.0

**Keys:** MW=Molecular Weight, Hydrogen bond acceptor, Hydrogen bond donor, MR=Molar Refractivity, TPSA=Topological Polar Surface Area

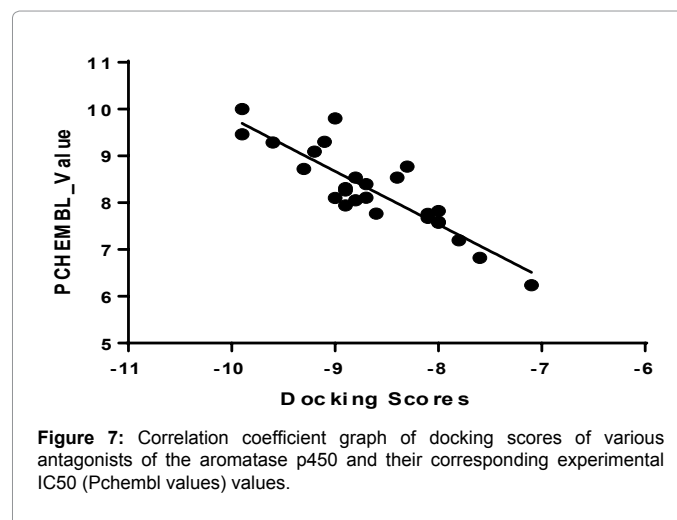
**Table 5:** Lipinski's drug-like properties of  $\alpha$ -selinene: The rule describes drug candidate's pharmacokinetics in the human body which also including their absorption, distribution, metabolism, and excretion ("ADME") using an online server (<http://www.scfbio-itt.res.in/>).

Predicted Physicochemical Properties of $\alpha$ -selinene					
<b>LogS (Solubility)</b>	<b>LogD<sub>7.4</sub></b> (Distribution Coefficient D)	<b>LogP</b> (Distribution Coefficient D)	LogS: Optimal: higher than -4 log mol/L LogD <sub>7.4</sub> : 1 to 3: Solubility moderate; Permeability moderate; Metabolism low. LogP: LogP >3: poor aqueous solubility		
-5.89 log mol/L	2.954	4.725			
Predicted Selected Absorption Properties of $\alpha$ -selinene					
<b>HIA</b> (Human Intestinal Absorption)	<b>F</b> (20% Bioavailability)	<b>F</b> (30% Bioavailability)	≥30%: HIA+; <30%: HIA- ≥20%: F20+; <20%: F20- ≥30%: F30+; <30%: F30		
0.877*	0.711*	0.54*			
Predicted Selected Distribution Properties of $\alpha$ -selinene					
<b>PPB</b> (Plasma Protein Binding)	<b>VD</b> (Volume Distribution)	<b>BBB</b> (Blood-Brain Barrier)	0.07-0.7L/kg: Evenly distributed BB ratio ≥0.1: BBB+; BB ratio <0.1: BBB		
75.9 %	0.42 L/kg	0.986*			
Predicted Selected Metabolism Properties of $\alpha$ -selinene					
P450 CYP3A4 inhibitor	P450 CYP3A4 substrate	P450 CYP2C9 inhibitor	P450 CYP2C9 substrate	P450 CYP2C19 inhibitor	P450 CYP2C19 substrate
0.04*	0.659*	0.02*	0.45*	0.215*	0.64*
Predicted Selected Elimination Properties of $\alpha$ -selinene					
<b>T<sub>1/2</sub></b> (Half Life Time)	<b>CL</b> (Clearance Rate)	Range: >8h: high; 3h < Cl < 8h: moderate; <3h: low Range: >15 mL/min/kg: high; 5mL/min/kg < Cl < 15mL/min/kg: moderate; <5 mL/min/kg: low			
1.871 h	1.853mL/min/kg				
Predicted Selected Toxicity Properties of $\alpha$ -selinene					
<b>H-HT</b> (Human Hepatotoxicity)	<b>AMES</b> (Ames Mutagenicity)	<b>LD50</b> (LD50 of acute toxicity)	High-toxicity: 1~50 mg/kg; Toxicity: 51~500 mg/kg; low-toxicity: 501~5000 mg/kg [34].		
0.236*	0.108*	4058.724 mg/kg			

\* Probability

**Table 6:** ADMET Evaluation properties of  $\alpha$ -selinene using online web-based server (<http://admet.scbdd.com/>)

when the docking scores of the compounds generated were plotted against chembl's pchem values (experimentally determined IC50) as indicated in Table 4 Figure 7. The reliability of our docking scores was further validated using the online available ChEMBL database; the FASTA sequence of the crystal structure of aromatase p450 was blasted on [www.ebi.ac.uk/chembl/](http://www.ebi.ac.uk/chembl/). The compounds obtained from the search were docked into the binding site of the aromatase p450, a correlation coefficient graph plotted between the docking scores of the compounds generated and their corresponding ChEMBL'S Pchem values



(experimentally determined IC50). This portrays a strong correlation coefficient between docking scores and the experimentally derived ones. Hence making computation experiment replicable and docking scores using PyRx autodock vina algorithm is dependable (Table 5).

## Conclusion

Docking studies and ADMET evaluation of  $\alpha$ -selinene with aromatase p450 showed that the ligand is a drug-gable molecule which plays critical role in the antagonism of aromatase p450, hence should be consider as a potential agent in breast cancer therapy (Table 6).

## References

1. Morounke SG, Ayorinde JB, Benedict AO, Adedayo FF, Adewale FO, et al. (2017) Epidemiology and Incidence of Common Cancers in Nigeria. J Cancer Biol Res 5: 1105.
2. Torre LA, Bray F, Siegel RL, Ferlay J, Lortet-Tieulent J, et al. (2015) Global cancer statistics, 2012. CA Cancer J Clin 65: 87-108.
3. Logan GJ, Dabbs DJ, Lucas PC, Jankowitz RC, Brown DD, et al. (2015) Molecular drivers of lobular carcinoma in situ. Breast Cancer Res 17: 76.
4. Wellings SR (1980) A hypothesis of the origin of human breast cancer from the terminal ductal lobular unit. Pathol Res Pract 166: 515-535.
5. Norton KA, Winger M, Bhanot G, Ganesan S, Barnard N, et al. (2010) A 2D mechanistic model of breast ductal carcinoma in situ (DCIS) morphology and progression. J Theor Biol 263: 393-406.
6. Inic Z, Zegarac M, Inic M, Markovic I, Kozomara Z, et al. (2014) Difference between luminal A and luminal B subtypes according to Ki-67, tumor size, and progesterone receptor negativity providing prognostic information. Clin Med Insights Oncol 8: 107-111.
7. Toft DJ, Cryns VL (2011) Minireview: basal-like breast cancer: from molecular profiles to targeted therapies. Mol Endocrinol 25: 199-211.
8. Brueggemeier RW, Hackett JC, Diaz-Cruz ES (2005) Aromatase inhibitors in the treatment of breast cancer. Endocr Rev 26: 331-345.
9. Caporuscio F, Rastelli G, Imbriano C, Del Rio A (2011) Structure-based design of potent aromatase inhibitors by highthroughput docking. J Med Chem 54: 4006-4017.
10. Stagg J, Andre F, Loi S (2012) Immunomodulation via chemotherapy and targeted therapy: a new paradigm in breast cancer therapy? Breast care (Basel) 7: 267-272.
11. Thompson Jr EA, Siiteri PK (1974) Utilization of oxygen and reduced nicotinamide adenine dinucleotide phosphate by human placental microsomes during aromatization of androstenedione. J Biol Chem 249: 5364-5372.
12. Chen SA, Besman MJ, Sparkes RS, Zollman S, Klisak I, et al. (1988) Human aromatase: cDNA cloning, Southern blot analysis, and assignment of the gene to chromosome 15. DNA 7: 27-38.
13. Akhtar M, Wright JN, Lee-Robichaud P (2011) A review of mechanistic studies on aromatase (CYP19) and 17 $\alpha$ -hydroxylase-17,20-lyase (CYP17) J Steroid Biochem Mol Biol 125: 2-12.
14. Harada N (1997) Aberrant expression of aromatase in breast cancer tissues. J Steroid Biochem Mol Biol 61: 175-184.
15. Lephart ED, Peterson KG, Noble JF, George FW, McPhaul MJ, et al. (1990) The structure of cDNA clones encoding the aromatase P-450 isolated from a rat Leydig cell tumor line demonstrates differential processing of aromatase mRNA in rat ovary and a neoplastic cell line. Mol Cell Endocrinol 70: 31-40.
16. Hammond ME, Hayes DF, Dowsett M, Allred DC, Hagerty KL (2010) American Society of Clinical Oncology/College Of American Pathologists guideline recommendations for immunohistochemical testing of estrogen and progesterone receptors in breast cancer. Arch Pathol Lab Med 134: e48-72.
17. Elledge RM, Green S, Pugh R, Allred DC, Clark GM, et al. (2000) Estrogen receptor (ER) and progesterone receptor (PgR), by ligand-binding assay compared with ER, PgR and pS2, by immunohistochemistry in predicting response to tamoxifen in metastatic breast cancer: a Southwest Oncology Group Study. Int J Cancer 89: 111-117.
18. Lockwood CA, Ricciardelli C, Raymond WA, Seshadri R, McCaul K, et al. (1999) A simple index using video image analysis to predict disease outcome in primary breast cancer. Int J Cancer 84: 203-208.
19. Panggabean G (1992) *Syzygium aqueum*, *Syzygium malaccense* & *Syzygium samarangense*: Edible fruits and nuts (2<sup>nd</sup> edn) Indonesia: Prosea Foundation Bogor, 292-294.
20. Osman H, Rahim AA, Isa NM, Bakhr NM (2009) Antioxidant activity and phenolic content of *Paederia foetida* and *Syzygium aqueum*. Molecules 14: 970-978.
21. Palanisamy UD, Ling LT, Manaharan T, Sivapalan V, Subramaniam T, et al. (2011) Standardized extract of *Syzygium aqueum*: A safe cosmetic ingredient. Int J Cosmet Sci 33: 269-275.
22. Tsuji-Naito K, Saeki H, Hamano M (2009) Inhibitory effects of Chrysanthemum species extracts on formation of advanced glycation end-products. Food Chem 116: 854-859.
23. Kawanishi Y, Noparatanawong S, Kamohara S, Nakano M (2003) Antioxidants supplementation prevents exercise induced oxidative damage in healthy subjects. J American Diabetes Association 103: 36.
24. Dent SF, Gaspo R, Kissner M, Pritchard KI (2011) Aromatase inhibitor therapy: toxicities and management strategies in the treatment of postmenopausal women with hormone-sensitive early breast cancer. Breast Cancer Res Treat 126: 295-310.
25. Amir E, Seruga B, Niraula S, Carlsson L, Ocaña A (2011) Toxicity of adjuvant endocrine therapy in postmenopausal breast cancer patients: a systematic review and meta-analysis. J Natl Cancer Inst 103: 1299-1309.
26. Beckwée D, Leysen L, Meuwis K, Adriaenssens N (2017) Prevalence of aromatase inhibitor-induced arthralgia in breast cancer: a systematic review and meta-analysis. Support Care Cancer 25: 1673-1686.
27. Rimawi MF and Osborne CK. Chapter 43: Adjuvant systemic therapy: endocrine therapy, in Harris JR, Lippman ME, Morrow M, Osborne CK. Diseases of the Breast, 5<sup>th</sup> edition. Lippincott Williams and Wilkins, 2014.
28. Adhikari N, Amin SA, Saha A, Jha T (2017) Combating breast cancer with nonsteroidal aromatase inhibitors (NSAIs): understanding the chemico-biological interactions through comparative SAR/QSAR study. Eur J Med Chem 137: 365-438.
29. Riemsma R, Forbes CA, Kessels A, Lykopoulos K, Amonkar MM (2010) Systematic review of aromatase inhibitors in the first-line treatment for hormone sensitive advanced or metastatic breast cancer, Breast Cancer Res. Treat 123: 9-24.